

Department of Pulmonary Medicine<sup>1</sup>, Xijing Hospital, Fourth Military Medical University, Xi'an; Genecast Cancer Precision Diagnosis and Treatment Center<sup>2</sup>, Wuxi, China

## Phillygenin regulates proliferation and apoptosis of non-small cell lung cancer through by AMPK/ERK/NF- $\kappa$ B axis

SHUO WU<sup>1, #</sup>, YAO ZHANG<sup>2, #</sup>, YAN ZHANG<sup>1</sup>, LIZHAN CHEN<sup>1</sup>, XI XU<sup>1</sup>, YINLI DANG<sup>1</sup>, XINYU TI<sup>1, \*</sup>

Received May 29, 2020, accepted July 3, 2020

\*Corresponding author: Xinyu Ti, Department of Pulmonary Medicine, Xijing Hospital, Fourth Military Medical University, Xi'an 710032, China  
ti\_xinyufmmu@126.com

#These authors contributed equally to this work.

Pharmazie 75: 512-515 (2020)

doi:10.1691/ph.2020.0558

An increasing number of studies have demonstrated that phillygenin (PG) exerts anti-oxidant, anti-inflammatory and anti-cancer activities. However, the effects of PG on the proliferation and invasion in non-small cell lung cancer (NSCLC) cells have not been clarified. In this study, MTT assay and flow cytometry were conducted to investigate the effect of PG on proliferation and apoptosis of NSCLC cells *in vitro*, respectively. A xenograft model of A549 cell was established in nude mice to validate the *in vitro* findings. Western blot were performed to measure the expression of molecules involved in AMPK/ERK/NF- $\kappa$ B pathway. Results suggested that PG (50 or 100  $\mu$ M) was significantly cytotoxic to A549 cells and SPC-A1 cells *in vitro*. PG treatment also inhibited the tumor growth of NSCLC cell mouse xenografts *in vivo*. These anti-proliferative and pro-apoptosis effects of PG were found to be regulated by the AMPK/ERK/NF- $\kappa$ B pathway. Consequently, PG suppressed proliferation and induced cell apoptosis in NSCLC cells. In conclusions, PG regulates AMPK/ERK/NF- $\kappa$ B axis in NSCLC cells, thereby inhibiting the proliferation and promoting the apoptosis of NSCLC cells.

### 1. Introduction

Lung cancer is one of the most commonly diagnosed malignancies, and ranks high in terms of both incidence and mortality (Zhao et al. 2020). Nearly 85% of the lung cancers cases are non-small cell lung cancer (NSCLC), which can be subdivided into adenocarcinoma, squamous cell carcinoma, large cell carcinoma and other types (Zhang et al. 2019). Given the effects of chemotherapy, surgery and radiotherapy, a remarkable reduction can be determined in the survival rate of NSCLC patients, in which the 5-year survival is still only 20.6% (Xu et al. 2018, 2019). However, traditional chemotherapy drugs have severe side effects and resistance, and increase treatment costs. To improve patient survival rate, a new effective drug for the treatment of NSCLC should be developed, and its exact mechanism also essential to be identified.

Phillygenin (PG), a tetrahydrofuran lignin, extracted from a traditional medical herb, *Forsythia suspensa*, is a relatively safe

drug with anticancer activity both *in vitro* and *in vivo* (Shen et al. 2019). Recent studies show that PG has multiple anticancer effects in some cancers. PG has been reported to inhibit *in vitro* and *in vivo* cancer cell growth in drug-resistant human esophageal cancer cells, through suppression of the ROS generation, mitochondrial membrane potential loss and promote tumor cell apoptosis and activation of the NF- $\kappa$ B signalling pathway (He et al. 2019). Hu et al. (2020) also found that PG can inhibit liver fibrosis through suppressing LPS-induced activation and inflammation by regulating the TLR4/MyD88/NF- $\kappa$ B pathway (Hu et al. 2020). In addition, PG processes its anti-inflammatory effect via modulating multiple cellular behaviors of mouse lymphocytes (Du et al. 2019). These studies substantiate that PG may play a vital role in lung-related disease. However, the effect of PG on the proliferation and apoptosis of NSCLC still remains unclear. Therefore, the present study was performed to investigate the effect of PG on the proliferation and apoptosis of NSCLC and the potential molecular mechanism.

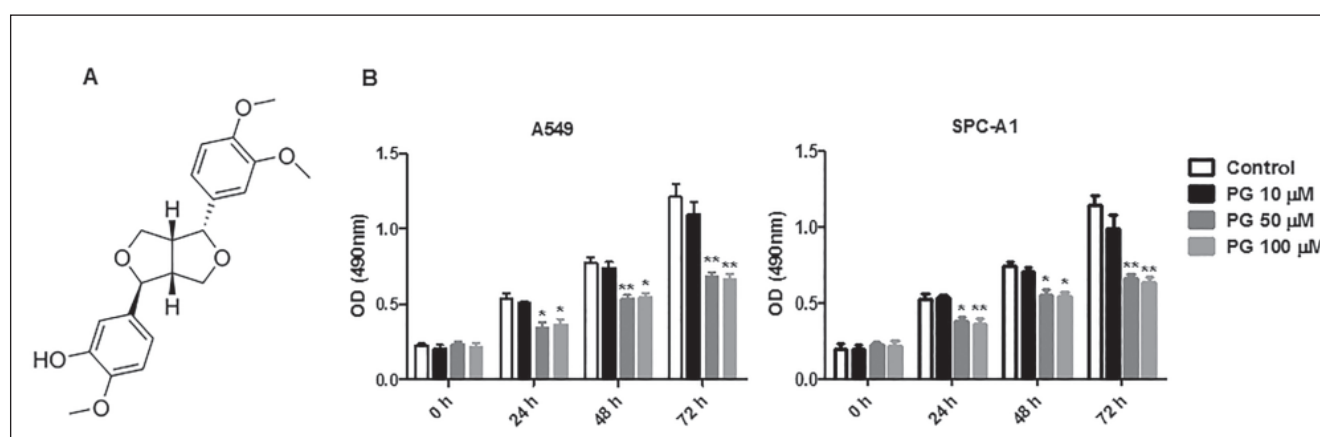


Fig. 1: Inhibitory effects of PG on cell viability in NSCLC cells. (A) Structure of PG and (B) Cell viability of A549 and SPC-A1 cells after PG treatment. Data are shown as mean $\pm$ SD. \*P < 0.05, \*\*P < 0.01, \*\*\*P < 0.001 vs control.

2. Investigations and results

2.1. Effect of PG on the viability in NSCLC cells in vitro

In this experiment, the effect of PG on the proliferation of NSCLC cells was detected by MTT assay. As shown in Fig. 1B, compared with the control group, the absorbance of A549 and SPC-A1 cells at 490 nm significantly decreased in a dose-dependent and time-dependent manner after PG treatment. According to the results of the MTT assay, the concentration of 50, 100 μM was selected for follow-up experimental conditions.

2.2. Effect of PG on the tumor growth in NSCLC cells in vivo

The tumour-bearing mouse model was used to examine the effect of proliferation with PG treatment *in vivo*. As shown in Fig. 2A, compared with the control group, the volume of tumours was significantly hampered by PG. Moreover, the weight of tumours was controlled by PG (Fig. 2B). These results suggested that PG inhibited tumor growth of NSCLC cells *in vivo*.

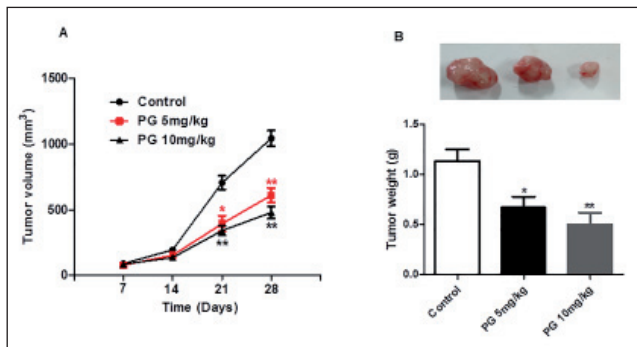


Fig. 2: Effects of PG on the growth of NSCLC cells *in vivo*. (A) The volume of tumours in the control group was significantly larger than in treatment groups 1. (B) The weight of tumours was also higher in the control group than in treatment groups. Data are shown as mean±SD. \*P < 0.05, \*\*P < 0.01 vs control.

2.3. Effect of PG on the apoptosis in NSCLC cells in vitro

To detect the apoptosis of A549 and SPC-A1, flow cytometry was used. As shown in Fig. 3A, compared with the control group, the apoptosis ratio of cells obtained through the flow cytometer was remarkably increased upon PG treatment. Moreover, PG also increased the apoptosis related protein, caspase-3 and Bax, associated with a decrease in Bcl-2 in both A549 and SPC-A1 cells (Fig. 3B). These findings suggested that PG could promote the apoptosis of NSCLC cells by regulating the expression of caspase-3, Bax and Bcl-2.

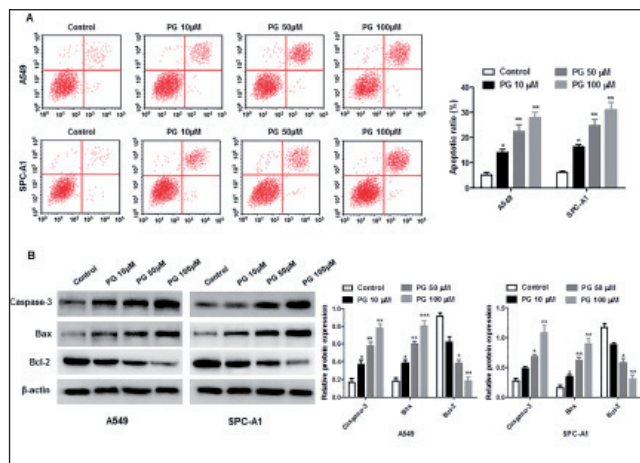


Fig. 3: PG induces apoptosis of NSCLC cells. Apoptosis and apoptotic-related proteins were detected in PG-treated A549 and SPC-A1 cells after 24 h treatment. (A) Flow cytometer (B) Western blot. Data are shown as mean±SD. \*P < 0.05, \*\*P < 0.01, \*\*\*P < 0.001 vs control.

2.4. Effect of PG on the AMPK, ERK, and NF-κB activation in NSCLC cells in vitro

To identify the mechanisms underlying cell apoptosis in PG-induced NSCLC cells, western blot was applied to measure the changes of related molecules upon PG treatment. PG treatment increased AMPK, ERK, and NF-κB phosphorylation in both A549 and SPC-A1 cells (Fig. 4).

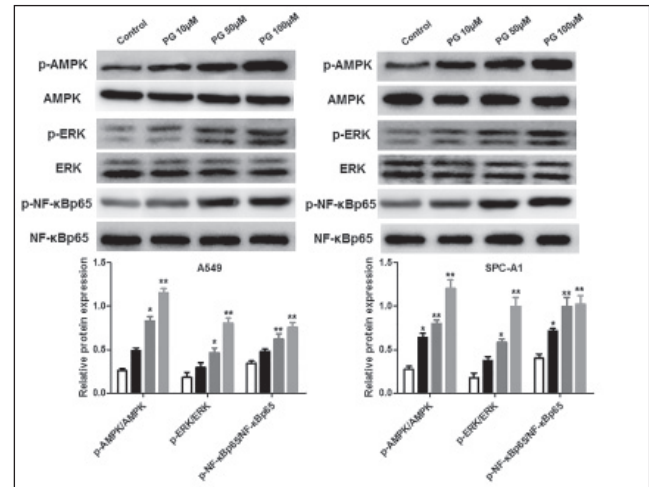


Fig. 4: PG increases phosphorylation of AMPK, ERK, and NF-κB in NSCLC cells. Phosphorylation levels of AMPK, ERK, and NF-κB were detected from PG-treated A549 and SPC-A1 cells by western blot analysis. Density of proteins was analyzed by Image J program. Data are shown as mean ± SD. \*P < 0.05, \*\*P < 0.01 vs control.

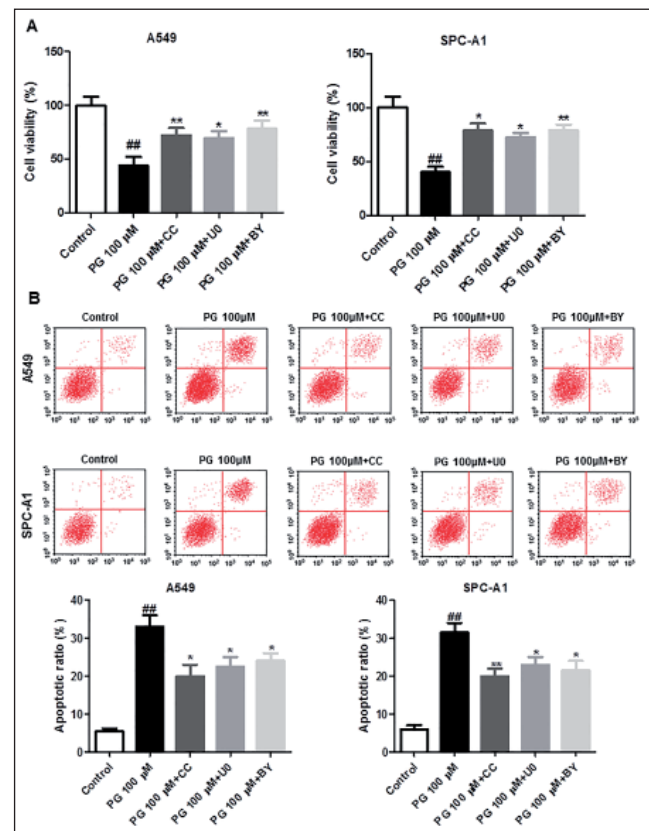


Fig. 5: PG-induced apoptosis of NSCLC cells is mediated via AMPK, ERK, and NF-κB signaling pathway. A549 and SPC-A1 cells were treated with PG 100 μM, compound C (CC), U0126 (UO), and BAY11-7082 (BY) for 24 h. (A) Cell viability of A549 and SPC-A1 cells after PG treatment. (B) Apoptosis were detected in PG-treated A549 and SPC-A1 cells after 24 h treatment. Data are shown as mean±SD. ##P < 0.01 vs control; \*P < 0.05, \*\*P < 0.01 vs PG 100 μM.

### 2.5. Effect of PG on the AMPK/ERK/NF- $\kappa$ B-mediated apoptosis in NSCLC cells in vitro

Based on the above research, the AMPK inhibitor, compound C (CC); ERK inhibitor, U0126 (U0); and NF- $\kappa$ B inhibitor, BAY11-7082 (BY) were employed to confirm the anti-proliferative and pro-apoptosis effects of PG on NSCLC cells. Co-treatment of CC, U0, or BY with 100  $\mu$ M PG increased the cell viability (Fig. 5A). Meanwhile, as shown in Fig. 5B, PG significantly increased the percentage of apoptotic cells in A549 and SPC-A1 cells, respectively; CC, U0, and BY co-treatments with PG decreased the apoptotic NSCLC cell percentage. Therefore, PG-induced apoptosis in NSCLC cells is mediated via AMPK/ERK/ NF- $\kappa$ B pathway.

### 3. Discussion

Lung cancer accounts for almost one-third of all cancer-related deaths, and despite the recent progress in therapeutic approaches, has unsatisfactory prognosis due to high recurrence and metastasis rates (Chen et al. 2015a, b). The incidence of lung cancer is increasing annually due to high levels of environmental pollution and a globally aging population. NSCLC is the predominant pathological type of lung cancer, and accounts for over 80% of all cases (Luo et al. 2020; Shi et al. 2020). Despite the current standard therapy, surgical resection combined with postoperative chemotherapy, the survival rate still remains unsatisfactory (Zhou et al. 2020). Drugs that are used in NSCLC chemotherapy generally cause side effects and injuries in normal tissues of cancer patients (Sier and Onugha 2020). Therefore, finding a potential treatment program to prevent and inhibit proliferation in NSCLC patients is necessary.

Traditional Chinese medicines have been shown to provide a rich resource for the identification of anticancer drugs (Li and Zhang 2020; Newman 2020). PG, a vital ingredient of the traditional Chinese herb *Forsythia suspensa*, has been reported to exert multiple anticancer effects in different cancers. However, few studies have focused on the anticancer effects of PG in NSCLC cells. Thus, we evaluated the anti-cancer effects of PG on A549 and SPC-A1 cell lines. We first found that PG could inhibit the proliferation of NSCLC cells. Results of subsequent experiments have shown that PG has excellent ability of promoting the apoptosis of NSCLC cells in a dose-dependent manner. Based on these results, we hypothesized that PG may inhibit the proliferation and promote the apoptosis of NSCLC cells.

In addition, many signaling pathways participate in tumor progression. Numbers of studies have reported that AMPK/ERK/NF- $\kappa$ B plays an important role in inflammation in the process of initiating oncogenic signal pathways in chronic inflammation, and can interact with each other to promote tumor proliferation, apoptosis and metastasis (Kinsey et al. 2019; Qin et al. 2019; Wang et al. 2019). AMPK activity can regulate the inflammatory response, and inactivation of AMPK promotes the development of inflammation (Banskota et al. 2015). NF- $\kappa$ B is a key molecule in the pro-inflammatory response. It can regulate the expression and function of various cytokines and chemokines, activate epithelial cell growth, and promote malignant transformation of tumor cells (Ding et al. 2020). ERK can activate NF- $\kappa$ B, further induce the expression of genes encoding apoptosis-inhibiting proteins, induce the expression of anti-apoptotic gene Bcl-2, and can promote apoptosis-inhibiting proteins (Wang et al. 2020). In the current study, PG treatment dose-dependently increased AMPK, ERK, and NF- $\kappa$ B phosphorylation, and their inhibitors blocked PG-induced apoptosis of NSCLC cells. Particularly, PG-decreased cell viability was increased by the AMPK inhibitor CC, ERK and NF- $\kappa$ B inactivation. We investigated the A549 and SPC-A1 cell viabilities after CC, U0, and BY treatment for 48 h. Thus, our findings support the conclusion that PG inhibits the proliferation of NSCLC cells through the AMPK/ERK/NF- $\kappa$ B signaling pathway.

In summary, PG can suppress the proliferation of NSCLC cells and promote apoptosis abilities. These effects are exerted by increasing the expression of caspase-3, Bcl-2, suppressing the expression of Bcl-2, and regulating the activity of the AMPK/ERK/NF- $\kappa$ B

signaling pathway. Thus, PG may be a potential anti-cancer agent for the treatment of NSCLC.

## 4. Experimental

### 4.1. Cell culture and treatment

Human NSCLC cell lines (A549 and SPC-A1 cells) were purchased from the Shanghai Cell Bank of Chinese Academy of Sciences (Shanghai, China). The above cells were cultured in DMEM (HyClone, New Zealand) containing 10% fetal bovine serum (FBS, Gibco Life Technologies, Carlsbad, USA) and a mixture of 1% streptomycin (100 U/mL) and penicillin (100  $\mu$ g/mL) (HyClone, New Zealand). The incubator with a humidified atmosphere of 5% CO<sub>2</sub> and 95% air was used for cell culture.

### 4.2. MTT assay

Cell viability was measured by MTT assay. In total,  $3 \times 10^3$  cells were seeded in each well of the 96-well plates and then placed in an incubator for overnight culture. The next morning, cells were treated with different concentrations of PG for 24, 48, and 72 h. Subsequently, 10  $\mu$ L of MTT (Solarbio, Beijing, China) solution was added into the well of the 96-well plates, and the cells were cultured for 4 h at 37 °C. The optical density of different groups was detected by using an enzyme immunoassay analyzer (Bio-Rad, Hercules, USA) at 490 nm. Cell viability was calculated using the following formula: cell viability (%) = experimental group absorbance value/control group absorbance value  $\times$  100%.

### 4.3. In vivo tumor growth model

Animal care and the experimental procedures were performed according to the guidelines established by the Animal Care and Ethics Committee of Xijing Hospital, Fourth Military Medical University. For tumor growth studies, BALB/c nude mice (4-6 weeks) (Vitalriver, Beijing, China) were subcutaneously injected with resuspended in Hank's buffer and mixed with equal volume of matrigel (BD Biosciences) with  $5 \times 10^6$  A549 cells and divided into control, 5 mg/kg PG, and 10 mg/kg PG treatment groups. Seven days after cell injection, PBS (20  $\mu$ L), GFP (5 or 10 mg/kg) was injected with tail vein every three days. Tumour volumes were measured with vernier calipers every seven days, and the tumours were removed and photographed on day 28.

### 4.4. Apoptosis assay

Cell apoptosis was assessed using an Annexin V-FITC/PI Apoptosis Kit (Solarbio Life Sciences, cat. no. CA1020). A549 and SPC-A1 cells were centrifuged after harvested. After washing, the cells were suspended in 1 $\times$  Binding buffer, and 100  $\mu$ L of cell suspension was mixed with 5  $\mu$ L of FITC and 5  $\mu$ L of PI. After incubation for 15 min in the dark, cell apoptosis was measured using a FACSCalibur flow cytometer (BD, FACSCalibur).

### 4.5. Western blot

The cells treated with PG for 48 h were collected and extracted with RIPA buffer (Beyotime Biotechnology, Shanghai, China), containing protease inhibitors and phosphatase (Roche Diagnostics, Indianapolis, IN, USA) inhibitors. The concentration of each sample was measured by using the BCA Protein Assay Kit (Beyotime Biotechnology, Shanghai, China). The protein solution was mixed with 5 $\times$ SDS buffer and boiled in boiling water for 5 to 10 min. Approximately 30  $\mu$ g of total protein in each sample was loaded in the lane, separated by SDS PAGE, and transferred to the polyvinylidene fluoride membrane (Millipore Corporation, Billerica, USA). The membranes were blocked by 5% skimmed milk, which was dissolved in 1 $\times$  TBST wash buffer, at room temperature for 2 h. Subsequently, these membranes were washed with 1 $\times$  TBST three times, each time for 10 min, and incubated overnight with the corresponding primary antibody at 4 °C according to the best dilution rate. The next morning, the membranes were washed with TBST and incubated with secondary antibodies. Immunoblots were performed using enhanced chemiluminescence-detecting substrate (Billerica, MA, USA). The protein expression levels were normalized to  $\beta$ -actin as an internal control.

### 4.6. Statistical analysis

The experimental data were analyzed by using SPSS 17.1 software and GraphPad Prism 5.0 software. All experiments were repeated three times and shown as mean  $\pm$  standard deviations (SD). Statistical analyses were performed using one-way ANOVA with Dunn's multiple comparisons test.  $P < 0.05$  was considered statistically significant.

Conflicts of interest: The authors declare that they have no competing interests.

## References

- Banskota S, Regmi SC, Kim JA (2015) NOX1 to NOX2 switch deactivates AMPK induces invasive phenotype in colon cancer cells through overexpression of MMP-7. *Mol Cancer* 14: 123.
- Chen L, Li X, Chen X (2015a) Prognostic significance of tissue miR-345 downregulation in non-small cell lung cancer. *Int J Clin Exp Med* 8: 20971–20976.
- Chen W, Zheng R, Baade PD, Zhang S, Zeng H, Bray F, Jemal A, Yu XQ, He J (2015b) Cancer statistics in China, 2015. *Ca Cancer J Clin* 66: 115–132.
- Ding J, Zhao J, Huan L, Liu Y, Qiao Y, Wang Z, Chen Z, Huang S (2020) Inflammation-induced LINC00665 increases the malignancy through activating PKR/NF- $\kappa$ B pathway in hepatocellular carcinoma. *Hepatology* doi: 10.1002/hep.31195

- Du B, Zhang L, Sun Y, Zhang G, Yao J, Jiang M, Pan L, Sun C (2019) Phillygenin exhibits anti-inflammatory activity through modulating multiple cellular behaviors of mouse lymphocytes. *Immunopharmacol Immunotoxicol* 41: 76–85.
- He J, Wei W, Yang Q, Wang Y (2019) Phillygenin exerts in vitro and in vivo antitumor effects in drug-resistant human esophageal cancer cells by inducing mitochondrial-mediated apoptosis, ROS generation, inhibition of the Nuclear Factor kappa B NF-kappaB signalling pathway. *Med Sci Monitor* 25: 739–745.
- Hu N, Wang , Dai X, Zhou M, Gong L, Yu L, Peng C, Li Y (2020) Phillygenin inhibits LPS-induced activation and inflammation of LX2 cells by TLR4/MyD88/NF-kappaB signaling pathway. *J Ethnopharmacol* 248: 112361.
- Kinsey CG, Camolotto SA, Boespflug AM, Guillen KP, Foth M (2019) Protective autophagy elicited by RAF-->MEK-->ERK inhibition suggests a treatment strategy for RAS-driven cancers. *Nat Med* 25, 620–627.
- Li B, Zhang W (2020) Chinese herbal formula Miao-Yi-Ai-Tang inhibits the proliferation and migration of lung cancer cells through targeting beta-catenin/AXIN and presents synergistic effect with cisplatin suppressing lung cancer. *Biomed Res Int* 2020: 2761850.
- Luo DB, Lv HB, Sun XH, Wang Y, Chu JH, Salai AL (2020) LncRNA TRERNA1 promotes malignant progression of NSCLC through targeting FOXL1. *Eur Rev Med Pharmacol Sci* 24: 1233–1242.
- Newman DJ (2020) Modern traditional Chinese medicine: identifying, defining and usage of TCM components. *Adv Pharmacol* 87: 113–158.
- Qin QF, Li SJ, Li YS, Zhang WK, Tian GH, Shang HC, Tang HB (2019) AMPK-ERK/CARM1 signaling pathways affect autophagy of hepatic cells in samples of liver cancer patients. *Frontiers Oncol* 9: 1247.
- Shen F, Wu W, Zhang M, Ma X, Cui Q, Tang Z, Huang H, Tong T, Yau L, Jiang Z, Hou Y, Bai G (2019) Micro-PET imaging demonstrates 3-O-beta-D-glucopyranosyl platycodigenin as an effective metabolite affects permeability of cell membrane and improves dosimetry of [ (18)F]-phillygenin in lung tissue. *Front Pharmacol* 10: 1020.
- Shi YB, Liu SL, Mou XR, Liao J, Che JP, Fei XQ, Wang AR (2020) Long noncoding RNA HOXA-AS2 acts as an oncogene by targeting miR-145-3p in human non-small cell lung cancer. *Eur Rev Med Pharm Sci* 24: 1243–1249.
- Sier R, Onugha O (2020) Review of procedures and outcomes of video-assisted thoracic surgery for the treatment of non-small cell lung cancer in 45 patients undergoing segmentectomy. *Surg Technol Int* 35: 36:245–250.
- Wang JC, Chen SY, Wang M, Ko JL (2019) Nickel-induced VEGF expression via regulation of Akt, ERK1/2, NFkappaB, AMPK pathways in H460 cells. 34: 652–658.
- Wang JR, Li TZ, Wang C, Li SM, Luo YH, Piao XJ, Feng YC, Zhang Y, Xu WT, Zhang Y, Zhang T, Wang SN, Xue H, Wang HX, Cao LK, Jin CH (2020) Liquiritin inhibits proliferation and induces apoptosis in HepG2 hepatocellular carcinoma cells via the ROS-mediated MAPK/AKT/NF-kappaB signaling pathway. *Naunyn Schmiedebergs Arch Pharmacol* 10.1007/s00210-019-01763-7.
- Xu BN, Zhang L, Zhang DD, Song CY, Tian DL, Jiang WJ (2018) Serum fork-head box D3 (FOXD3) expression is down-regulated in and associated with diagnosis of patients with non-small cell lung cancer. *Med Sci Monitor* 24: 9504–9508.
- Xu S, Lam SK, Cheng PN, Ho JC (2019) Contactin 1 modulates pegylated arginine resistance in small cell lung cancer through induction of epithelial-mesenchymal transition. *Sci Rep* 9: 12030.
- Zhang R, Tao F, Ruan S, Hu M, Hu Y, Fang Z, Mei L, Gong C (2019) The TGFbeta1-FOXM1-HMGA1-TGFbeta1 positive feedback loop increases the cisplatin resistance of non-small cell lung cancer by inducing G6PD expression. *Am J Transl Res* 11: 6860–6876.
- Zhao D, Liu H, Liu H, Zhang X, Zhang M, Kolluri VK, Feng X, He Z, Wang M, Zhu T, Yan X, Zhou Y (2020) Downregulated expression of hsa\_circ\_0037515 and hsa\_circ\_0037516 as novel biomarkers for non-small cell lung cancer. *Am J Transl Res* 12: 162–170.
- Zhou W, Zhang W, Han B (2020) [Studies and progress of EGFR exon 20 insertion mutation in non-small cell lung cancer]. *Zhongguo fei ai za zhi = Chin J Lung Cancer* 23: 118–126.